Vertica, 1977, Vol. 1, pp. 291–306. Pergamon Press. Printed in Great Britain

SEMI-ANALYTIC METHODS FOR FREQUENCIES AND MODE SHAPES OF ROTOR BLADES

V. GIURGIUTIU* and R. O. STAFFORD

Aeronautics Department, Imperial College, London SW7, England

(*Received January; received for publication* 14 *April* 1977)

Abstract—The equations of motion including shear and rotatory inertia are developed for coupled linear lag, flap and pitch vibrations of blades rotating at constant angular velocity in a fixed plane. For uncoupled motions three ordinary differential equations are obtained for the shape functions, and a solution is obtained in terms of four independent functions, each a convergent power series. These rotating beam functions are similar to classic normal beam functions, and transfer matrices are used to treat piecewise uniform blades. The simplicity and accuracy of the method is illustrated with spoke diagrams and moment and shear curves of typical rotor blades.

NOMENCLATURE

A_n, A_k^i	coefficients in the power series expansion
a, b, c	coefficients of quadratic axial force
B_k	matrix of beam functions
C_i	constants to be determined from boundary conditions
d	displacement vector
D	transfer matrix for the whole blade
E, G	elastic moduli
f	force vector
$F_i(\xi)$	beam function
κ_ϕ	root torsion stiffness, Nm/rad.
k_1, k_2	shear deflection coefficients
l_i	length of a beam segment, m
m	distributed mass, kg/m
M_η, M_ζ	bending moments, Nm
M_x	torque, Nm
M	concentrated mass, kg
P_i	point transfer matrix
p_x, p_y, p_z	distributed loads, N/m
q_x, q_y, q_x	distributed moment loading, N
R	blade tip radius
S_η, S_ζ	shear stress resultants, N
T	blade torsion, N
U_i	transfer matrix over the i^{th} segment
u, v, w	displacements of the elastic axis
v_b, w_b, v_s, w_s	positions of v, w due to bending and shear
x, y, z	rotating coordinate system defining the plane of rotation
x, η, ζ	rotating coordinate system defining the undeformed blade principal axes
α_v, α_w, α_ϕ	nondimensional rotation speed coefficients
δ_v, δ_w	nondimensional shear deflection coefficients
ϵ_{xx}, $\epsilon_{x\eta}$, $\epsilon_{x\zeta}$	engineering strain components
θ	blade pitch angle, rad.
$\lambda(\eta,\zeta)$	warping function
Λ	ratio of structural and mass radii of gyration
τ	nondimensional axial force
μ_v, μ_w, μ_ϕ, μ_{12}	nondimensional inertia coefficients
ξ	dimensionless axial coordinate
σ_{xx}, $\sigma_{x\eta}$, $\sigma_{x\zeta}$	engineering stress, N/m^2
ϕ	torsion deflection, rad.
$(\,)'$	$\partial/\partial x$ or $\partial/\partial \xi$
$(\dot{\,})$	$\partial/\partial t$
ω	natural frequency, rad/sec.
Ω	rotation speed, rad/sec.

* Present address: Institutul de Mecanica Fluidelor si Constructii Aerospatiale, Bucharest, Romania.

1. INTRODUCTION

In a previous paper [1] the uncoupled lag and flap equations for Timoshenko beams were derived, and solutions were obtained with the Frobenius power series method. Those results are extended here by deriving a slightly modified set of the general linear equations for coupled bending and torsional vibrations. This derivation differs from the classic equations [2,3] only in that principal axes are used. Principal axes derivations retain the difference between flatwise and chordwise deformations and hence are useful for order-of-magnitude studies. Though the resulting equations couple only through the inertia terms, the simplicity of the stress resultants is balanced by the complexity of the accelerations.

As before the goal is to solve exactly the uncoupled equations for lag, flap and pitch vibrations of piecewise uniform rotor blades. In Section 2, the equations of motion are briefly derived in principal axes, including shear deflection and rotatory inertia terms. Assumptions are introduced which lead to uncoupled equations, and a slightly nonstandard set of dimensionless coefficients is introduced to allow treatment of both stationary and rotating beams. For steady free vibrations, ordinary differential equations are obtained and solved in Section 3 by the Frobenius method. The result is a set of explicit polynomials generated by recursion formulae. These polynomials are the "beam functions" for rotating beams, and are treated like any known function. A transfer matrix is defined in Section 4 which allows one to readily formulate problems describing non-uniform blades in terms of piecewise uniform segments. Application of boundary conditions leads to a small (2 × 2) determinant whose roots are the frequencies. Two examples are presented in Section 5 to illustrate the spoke diagrams, mode shapes, moments and shears of typical blades. A brief comparison is made with a commonly used empirical formula [4]. Full details of a parameter study and convergence of the bending solutions were given in [1].

2. THE EQUATIONS OF MOTION

Attention is restricted to a pitched uniform rotor blade of zero pre-twist and zero pre-cone (Fig. 1.) A symmetric airfoil section is employed and the centres of shear, mass and tension are assumed to coincide.

First order strain–displacement relations will be considered, but the shear and rotary inertia corrections [5] to Euler's Theory of Bending (henceforth ETB) are included. Hence the bending displacements of the principal axes, v, w, are split into contributions due to bending (subscript b) and due to shear (subscript s)

$$v = v_s + v_b, \qquad w = w_s + w_b \tag{1}$$

Thus the usual strain–displacement relations become

$$\begin{aligned} \epsilon_{xx} &= u' - v_b''\eta - w_b''\zeta, \\ \epsilon_{x\eta} &= -\left(\zeta + \frac{\partial\lambda}{\partial\eta}\right)\phi' + v_s', \\ \epsilon_{x\zeta} &= \left(\eta - \frac{\partial\lambda}{\partial\zeta}\right)\phi' + w_s'. \end{aligned} \tag{2}$$

where λ is the warping function of St. Venant's torsion theory. The first terms in $\epsilon_{x\eta}$ and $\epsilon_{x\zeta}$ represent the effect of torsion, the second terms the effect of shear. The material is considered isotropic and elastic, hence

$$\sigma_{xx} = E\epsilon_{xx}, \qquad \sigma_{x\eta} = G\epsilon_{x\eta}, \qquad \sigma_{x\zeta} = G\epsilon_{x\zeta}. \tag{3}$$

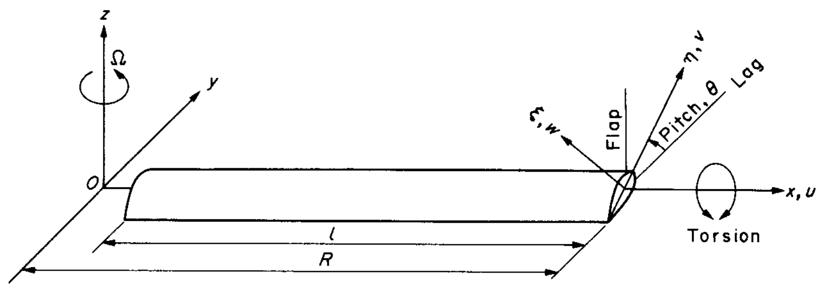

Fig. 1. Orientation and motion of a pitched uniform blade.

Consideration of force and moment equilibrium for the differential elements in Fig. 2 results in the following first order equations:

$$
\begin{aligned}
T' + p_x &= 0,\\
S_\eta' + (Tv')' + p_\eta &= 0,\\
S_\zeta' + (Tw')' + p_\zeta &= 0,\\
M_x' + q_x &= 0,\\
M_\eta' + S_\zeta + q_\eta &= 0,\\
M_\zeta' + S_\eta + q_\zeta &= 0,
\end{aligned}
\tag{4}
$$

where p_x, p_η, p_ζ, and q_x, q_η, q_ζ, represent the distributed applied forces and moments. By combining (2) with (3) and integrating over the cross-section, the stress resultants in (4) are obtained for a Timoshenko beam with axial load [3].

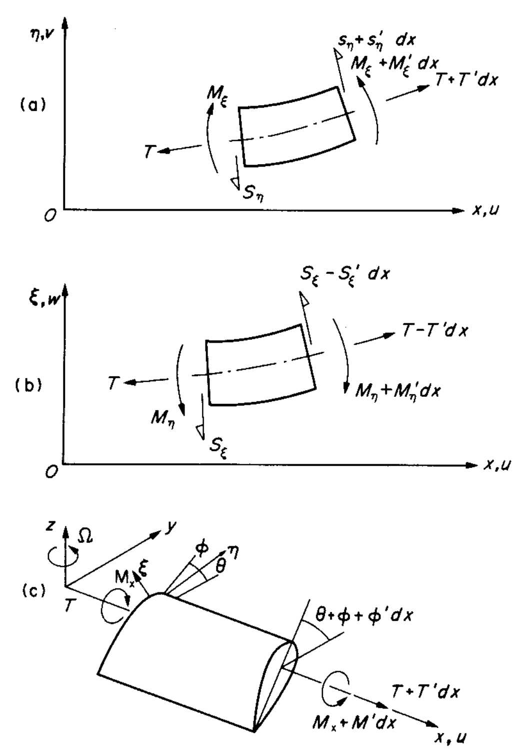

Fig. 2. Differential elements: (a) flatwise (b) chordwise, and (c) torsion.

$$T = \iint_A \sigma_{xx}\,\mathrm{d}A = EAu'$$

$$S_\eta = \iint_A \sigma_{x\eta}\,\mathrm{d}A = Gk_1Av_s', \quad S_\zeta = \iint_A \sigma_{x\zeta}\,\mathrm{d}A = Gk_2Aw_s',$$

$$M_\eta = \iint_A \sigma_{xx}\zeta\,\mathrm{d}A = -EI_1w_b'', \qquad M_\zeta = -\iint_A \sigma_{xx}\eta\,\mathrm{d}A = EI_2v_b'', \tag{5}$$

$$M_x = \iint_A (\eta\sigma_{x\zeta} - \zeta\sigma_{x\eta})\,\mathrm{d}A + \iint_A (\eta^2 + \zeta^2)\sigma_{xx}\phi'\,\mathrm{d}A$$

$$= GJ\phi' + k_A^2T\phi',$$

where

$$EA = \iint_A E\,\mathrm{d}A, \qquad EI_1 = \iint_A E\zeta^2\,\mathrm{d}A, \qquad EI_2 = \iint_A E\eta^2\,\mathrm{d}A,$$

$$GJ = \iint_A G\left(\eta^2 + \zeta^2 - \eta\frac{\partial\lambda}{\partial\zeta} + \zeta\frac{\partial\lambda}{\partial\eta}\right)\mathrm{d}A$$

are the usual elastic constant of the section, k_1 and k_2 are the shear deflection coefficients, and

$$k_A^2 = \frac{1}{A}\iint_A (\eta^2 + \zeta^2)\mathrm{d}A$$

is the area radius of gyration. The first integral in the last of (5) is the usual St. Venant torsional stiffness, and the second integral represents the untwisting effects of longitudinal stress [2]. Second order warping effects [6], and coupling between warping and shear resultants are ignored.

For free vibrations the loads are solely inertial and are derived from the acceleration components. Consider an element of mass $\rho\mathrm{d}A$ initially at position (x, η, ζ). After deformation its vector position in the original frame is

$$\mathbf{t}_1 = [\mathbf{i}\,\mathbf{j}\,\mathbf{k}]\left\{\begin{bmatrix} x + u \\ v \\ w \end{bmatrix} + \begin{bmatrix} 1 & -v_b' & -w_b' \\ v_b' & 1 & \phi \\ w_b' & -\phi & 1 \end{bmatrix}\begin{bmatrix} 0 \\ \eta \\ \zeta \end{bmatrix}\right\}. \tag{6}$$

The expression for acceleration vector in a rotating frame is used

$$\boldsymbol{\sigma} = \ddot{\mathbf{t}}_1 + 2\omega \times \dot{\mathbf{r}}_1 + \omega \times (\omega \times \mathbf{r}_1), \tag{7}$$

where the rotation vector is

$$\omega = \Omega\sin\theta\,\mathbf{j} + \Omega\cos\theta\,\mathbf{k}. \tag{8}$$

Substituting (6) and (8) into (7) and performing the vector products yields the expressions for the acceleration components

$$\begin{aligned} a_x &= \ddot{u} - \eta\ddot{v}_b' - \zeta\ddot{w}_b' + 2\Omega[-\dot{v}\cos\theta + \dot{w}\sin\theta + \dot{\phi}(\eta\sin\theta + \zeta\cos\theta)] \\ &\quad - \Omega^2(x + u - \eta v_b' - \zeta w_b'), \\ a_\eta &= \ddot{v} - \zeta\ddot{\phi} + 2\Omega(\dot{u} - \eta\dot{v}_b' - \zeta\dot{w}_b')\cos\theta + \Omega^2[(w + \zeta)\sin\theta\cos\theta \\ &\quad - (v + \eta)\cos^2\theta + \phi(\eta\sin\theta\cos\theta + \zeta\cos^2\theta)], \\ a_\zeta &= \ddot{w} + \eta\ddot{\phi} - 2\Omega(\dot{u} - \eta\dot{v}_b' - \zeta\dot{w}_b')\sin\theta + \Omega^2[-(w + \zeta)\sin^2\theta \\ &\quad + (v + \eta)\sin\theta\cos\theta - \phi(\eta\sin^2\theta + \zeta\sin\theta\cos\theta)]. \end{aligned} \tag{9}$$

Hence the inertial forces and moments are evaluated in a d'Alembert sense, and to first order in displacements they are

$$
\begin{aligned}
p_x &= -\iint_A \rho a_x \,\mathrm{d}A = -m\ddot{u} + 2m\Omega(\dot{v}\cos\theta - \dot{w}\sin\theta) + m\Omega^2(x+u),\\
p_\eta &= -\iint_A \rho a_\eta \,\mathrm{d}A = -m\ddot{v} - 2m\Omega\dot{u}\cos\theta + m\Omega^2\cos\theta(v\cos\theta - w\sin\theta)\\
p_\zeta &= -\iint_A \rho a_\zeta \,\mathrm{d}A = -\mathrm{m}\ddot{w} + 2m\Omega\dot{u}\sin\theta - m\Omega^2\sin\theta(v\cos\theta - w\sin\theta)\\
q_x &= -\iint_A \rho[a_\zeta(\eta - v) - a_\eta(\zeta - w)]\,\mathrm{d}A = -mk_m^2\ddot{\phi} - 2m\Omega(k_{m_1}\dot{w}_b'\cos\theta\\
&\quad + k_{m_2}^2\dot{v}_b'\sin\theta) - m\Omega^2(k_{m_2}^2 - k_{m_1}^2)\phi\cos 2\theta - \tfrac{1}{2}m\Omega^2(k_{m_2}^2 - k_{m_1}^2)\sin 2\theta,\\
q_\eta &= -\iint_A \rho a_x(\zeta - w)\,\mathrm{d}A = mk_{m_1}^2(-\ddot{w}_b' + \Omega^2 w_b' + 2\Omega\dot{\phi}\cos\theta),\\
q_\zeta &= \iint_A \rho a_x(\eta - v)\,\mathrm{d}A = mk_{m_2}^2[(-\ddot{v}_b' + \Omega^2 v_b') + 2\Omega\dot{\phi}\sin\theta],
\end{aligned}
\tag{10}
$$

where

$$
m = \iint_A \rho\,\mathrm{d}A,\qquad k_{m_1}^2 = \frac{1}{m}\iint_A \rho\zeta^2\,\mathrm{d}A,\qquad k_{m_2}^2 = \frac{1}{m}\iint_A \rho\eta^2\,\mathrm{d}A,\qquad k_m^2 = k_{m_1}^2 + k_{m_2}^2
$$

are the section inertial constants. Substitution of (5) and (10) into (4) yields the coupled differential equations of motion

$$
\begin{aligned}
&T' - m\ddot{u} + 2m\Omega(\dot{v}\cos\theta - \dot{w}\sin\theta) + m\Omega^2 u = -m\Omega^2 x,\\
&EI_2 v_b'''' - (Tv')' + mk_{m_2}^2(-\ddot{v}_b'' + \Omega^2 v_b'' + 2\Omega\dot{\phi}'\sin\theta) + m\ddot{v}\\
&\qquad + 2m\Omega\dot{u}\cos\theta - m\Omega^2\cos\theta\,(v\cos\theta - w\sin\theta) = 0,\\
&EI_1 w_b'''' - (Tw')' + mk_{m_1}^2(-\ddot{w}_b'' + \Omega^2 w_b'' + 2\Omega\dot{\phi}'\cos\theta)\\
&\qquad + m\ddot{w} - 2m\Omega\dot{u}\sin\theta + m\Omega^2\sin\theta\,(v\cos\theta - w\sin\theta) = 0,\\
&GJ\phi'' + k_A^2(T\phi')' - mk_m^2\ddot{\phi} + 2m\Omega(k_{m_1}^2\dot{w}_b'\cos\theta + k_{m_2}^2\dot{v}_b'\sin\theta)\\
&\qquad - m\Omega^2(k_{m_2}^2 - k_{m_1}^2)\phi\cos 2\theta = -\tfrac{1}{2}m\Omega^2(k_{m_2}^2 - k_{m_1}^2)\sin 2\theta.
\end{aligned}
\tag{11}
$$

The first and last of (11) describe axial and torsional vibrations which couple with bending via Coriolis terms; the second and third describe chordwise and flatwise bending, respectively.

These equations are coupled by both centrifugal and Coriolis effects, but the Coriolis terms are much the smaller. For practical rotor blades the axial stiffness is very large and axial displacements can be shown to be two orders of magnitude smaller than the bending displacements. Hence the contribution of u and its time derivatives to the inertia loading is ignored. In the bending equations the remaining Coriolis terms modify the rotatory inertia contribution. However $\Omega\dot{\phi}'/\Omega^2 w_b''$ is of order k_m/R, the mass radius of gyration. Likewise, $\Omega\dot{w}_b'/\Omega^2\phi$ is of order $R^4\sqrt{(m\omega^2/EI)}$ which is small for the bending frequencies considered. Hence the Coriolis terms in $(11)_{2,3,4}$ will be ignored.*

Our immediate purpose is to derive "beam functions" for rotating beams, and for this it is convenient to uncouple the equations by setting the pitch angle θ to zero.

*An extensive order-of-magnitude study is given in [3].

Using (1) and (5) to write v_b and w_b in terms of total displacements, the uncoupled equations become

$$T' = -m\Omega^2 x, \tag{12a}$$

$$EI_2 v'''' - (Tv')' + m(\ddot{v} - \Omega^2 v) + \frac{EI_2}{Gk_1A}[-m(\ddot{v} - \Omega^2 v)'' + (Tv')''']$$

$$-mk_{m_2}^2(\ddot{v} - \Omega^2 v)'' + \frac{mk_{m_2}^2}{Gk_1A}\{m(\ddot{\ddot{v}} - 2\Omega^2\ddot{v} + \Omega^4 v) - [T(\ddot{v} - \Omega^2 v)']'\} = 0, \tag{12b}$$

$$EI_1 w'''' - (Tw')' + m\ddot{w} + \frac{EI_1}{Gk_2A}[-m\ddot{w}'' + (Tw')'''] - mk_{m_1}^2(\ddot{w} - \Omega^2 w)''$$

$$+\frac{mk_{m_1}^2}{Gk_2A}\{m(\ddot{\ddot{w}} - \Omega^2\ddot{w}) - [T(\ddot{w} - \Omega^2 w)']'\} = 0, \tag{12c}$$

$$GJ\phi'' + k_A^2(T\phi')' - mk_m^2\ddot{\phi} - m\Omega^2(k_{m_2}^2 - k_{m_1}^2)\phi = 0. \tag{12d}$$

Since u has been ignored (12a) yields the steady axial tension in form

$$T(x) = T_0 - \tfrac{1}{2}m\Omega^2 x. \tag{13}$$

Bending and torsional vibrations are assumed to be steady and harmonic, and separation of variables is implied by the substitution $\partial/\partial t = iw$. It is convenient to use the following dimensionless coefficients:

	Lag	Flap	Torsion	
Rotation speed:	$\alpha_v = \dfrac{ml^4\Omega^2}{EI_2}$	$\alpha_w = \dfrac{ml^4\Omega^2}{EI_1}$	$\alpha_\phi = \dfrac{ml^4\Omega^2}{GJ}$	
Frequency:	$\lambda_v = \dfrac{ml^4\omega^2}{EI_2}$	$\lambda_w = \dfrac{ml^4\omega^2}{EI_1}$	$\lambda_\phi = \dfrac{ml^4\omega^2}{GJ}$	(14)
Inertia:	$\mu_v = k_{m_2}^2/l^2$	$\mu_w = k_{m_1}^2/l^2$	$\mu_\phi = \mu_v + \mu_w$ $\mu_{12} = \mu_w - \mu_v$	
Shear deflection:	$\delta_v = \dfrac{EI_2}{Gk_1Al^2}$	$\delta_w = \dfrac{EI_1}{Gk_2Al^2}$	N.A.	

The ratio of structural and mass radii of gyration is denoted by

$$\Lambda = k_A^2/k_m^2 \tag{15}$$

The dimensionless speed parameters are chosen with Ω in the numerator so that both operational and zero speed conditions can be accommodated. The remaining parameters in (14), except frequency, are usually small for practical configurations.

The axial coordinate is made dimensionless by defining $\xi = x/l$, and henceforth $(\ )'$ denotes $d/d\xi$. The dimensionless axial force is defined by

$$\tau(\xi) = T(x)/m\Omega^2 l^2 \tag{16}$$

but the deflections v, w, and ϕ, are kept in dimensional form to facilitate matching boundary conditions between discontinuous segments. Hence substitution of (14), (15) and (16) into (12) yields the set of ordinary differential equations for the mode shapes.

$$(1 + \delta_v\alpha_v\tau)v'''' + 3\delta_v\alpha_v\tau v''' - [1 - \mu_v\delta_v(\lambda_v + \alpha_v)] \times [\alpha_v\tau' v' + (\lambda_v + \underline{\alpha_v})v] + [\mu_v(1 + \delta_v\alpha_v\tau)(\lambda_v + \alpha_v) + \delta_v(\lambda_v + \underline{\alpha_v}) - \alpha_v(\tau - 3\delta_v\tau'')]v'' = 0, \quad (17a)$$

$$(1 + \delta_w\alpha_w\tau)w'''' + 3\delta_w\alpha_w\tau w''' - [1 - \mu_w\delta_w(\lambda_w + \alpha_w)] \times (\alpha_v\tau' w' + \lambda_w w) + [\delta_w\alpha_w + \mu_w(1 + \delta_w\alpha_w\tau)(\lambda_w + \alpha_w) - \alpha_w(\tau - 3\delta_w\tau'')]w'' = 0, \quad (17b)$$

$$\phi'' + \Lambda\mu_\phi\alpha_\phi(\tau\phi')' + (\lambda_\phi\mu_\phi - \alpha_\phi\mu_{12})\phi = 0. \quad (17c)$$

The only difference between the lag and flap equations lies in terms from the lateral effect of centrifugal force shown underlined in (17a).

3. SOLUTION BY THE FROBENIUS METHOD

Since (17a–c) are linear real ordinary differential equations, the solution can be expressed in terms of real positive integer powers of the independent variable [7] in the form

$$X(\xi) = \sum_{n=0}^{\infty} A_n \xi^{n+p} \quad (18)$$

where the dependent variable $X(\xi)$ may be either $v(\xi)$, $w(\xi)$ or $\phi(\xi)$. The dimensionless axial force (13) is written in a general form

$$\tau(\xi) = a + b\xi + c\xi^2. \quad (19)$$

For discontinuous beams, or beams with concentrated inertias, constants a, b, and c, will also be discontinuous.

The constant exponent in (18) has to be determined from the indicial equation [7]. Inspection of (17a) and (17b) indicates that these equations have no singular points. Thus for the bending solutions p is zero. Examination of the torsion equation (17c) indicates the possibility of regular singular points, but for practical multi-segmented configurations, they are outside the range of interest $0 < \xi < 1$. In the case of a uniform shaft-fixed cantilever it can be shown [4] that (17c) has a regular singularity at $\xi = 1$ and through a simple transformation of independent variables, it becomes the Legendre equation, for which the series solution is again (18) with $p = 0$ [8]. Thus solutions of (17) can be sought with the Maclaurin expansion

$$X(\xi) = \sum_{n=0}^{\infty} A_n \xi^n. \quad (20)$$

Due to the similarity of (17a) and (17b), the derivation of their solutions can be unified. Substitution of (19) and (20) into (17a) and collection of the coefficients of like powers of ξ yield the following recurrence relation for the lag motion,

$$(1 + \alpha_v\delta_v a)A_{n+4} = -\frac{\alpha_v\delta_v b(n+3)A_{n+3}}{n+4} - [\delta_v(\lambda_v + \underline{\alpha_v}) - \alpha_v a + \mu_v(\lambda_v + \alpha_v)(1 + \alpha_v\delta_v a) + (n+3)(n+2)\alpha_v\delta_v c]\frac{A_{n+2}}{(n+4)(n+3)} + [1 - \mu_v\delta_v(\lambda_v + \alpha_v)]\frac{(n+1)^2\alpha_v b A_{n+1} - [\lambda_v + \underline{\alpha_v} + n(n+1)\alpha_v c]A_n}{(n+4)(n+3)(n+2)(n+1)},$$

$$n \geqslant 0. \quad (21)$$

Similar substitution into (17b) yields an expression for the flap motion which is obtained from (21) by deletion of the terms underlined and appropriate replacement of the constants. Hence the development of the two bending solutions can proceed together.

Inspection of (21) shows that only four coefficients can be chosen arbitrarily, and these are taken to be A_0 through A_3. Hence four independent functions are defined as follows

$$F_i(\xi) = \xi^{i-1} + \sum_{n=4}^{\infty} A_n^i \xi^n, \qquad i = 1, \ldots, 4. \tag{22}$$

Thus the four independent sets of A^i are obtained from (21) by using the following initial values:

For $F_i(\xi)$ set

$$A_{i-1}^i = 1, \text{ and } A_k^i = 0, k = 0, 1, 2, 3 \text{ but } k \neq i - 1. \tag{23}$$

For example, to generate $F_3(\xi)$, set

$$A_0^3 = A_1^3 = A_3^3 = 0 \quad \text{and} \quad A_2^3 = 1.$$

Then (21) is used to generate the remaining terms.

The general solution of (17a) and (17b) can now be written as

$$v(\xi), w(\xi) = C_1 F_1(\xi) + C_2 F_2(\xi) + C_3 F_3(\xi) + C_4 F_4(\xi) \tag{24}$$

where constants C_i are determined from the boundary conditions.

Inspection of (21) shows that at $\xi = 1$ only two terms need be examined to establish convergence,

$$A_{n+4} = -\frac{\alpha_v \delta_v b(n+3) A_{n+3}}{(1 + \alpha_v \delta_v a)(n+4)} - \frac{\alpha_v \delta_v c(n+2) A_{n+2}}{(1 + \alpha_v \delta_v a)(n+4)}$$

$$+ \text{(strongly convergent terms)}, \qquad \alpha_v \delta_v = \frac{m(l\Omega)^2}{G k_1 A}. \tag{25}$$

To ensure rapid convergence the terms $\alpha_v \delta_v b$, $\alpha_v \delta_v c$, and the corresponding terms for flap motion must be small, and for most rotor blades log $(\alpha_v \delta_v) < -1$. For very large speeds $\alpha_v \delta_v$ and $\alpha_w \delta_w$ can always be made small by subdividing the blade into two or more segments, so that $l\Omega$ is small (this was found necessary for aeroplane propellers [9]). Convergence of the higher derivatives (up to the third are required in the boundary conditions) is established by similar arguments.

In the degenerate case of no rotation and zero shear deformation and rotatory inertia, the recurrence formula (21) reduces to

$$A_{n+4} = \frac{n!}{(n+4)!} \lambda_v A_n, \qquad \lambda_v = (\beta_1 l)^4.$$

Using (23), functions (22) reduce to

$$F_1 = (\cos \beta_1 x + \cosh \beta_1 x)/2, \qquad F_2 = (\sin \beta_1 x + \sinh \beta_1 x)/2\beta_1 l,$$

$$F_3 = (-\cos \beta_1 x + \cosh \beta_1 x)/(\beta l)^2, \qquad F_4 = (-\sin \beta_1 x + \sinh \beta_1 x)/[(\beta l)^3/3].$$

The denominators can be combined with the constants C_i in (24) and the usual non-rotating beam bending functions [5] are recovered.

Since (17c) is a second order differential equation, the torsion equation yields a much simpler recurrence formula,

$$A_{n+2} = -\frac{(n+1)^2 \Lambda\mu_\phi\alpha_\phi b A_{n+1} + [n(n+1)\Lambda\mu_\phi\alpha_\phi c + \lambda_\phi\mu - \alpha_\phi\mu_{12}]A_n}{(n+2)(n+1)(1+\Lambda\mu_\phi\alpha_\phi a)}. \quad (26)$$

The torsional equivalents of (22) and (24) are

$$F_i(\xi) = \xi^{i-1} + \sum_{n=2}^{\infty} A_n^i \xi^n, \qquad i = 1, 2, \quad (27)$$

$$\phi(\xi) = C_1 F_1(\xi) + C_2 F_2(\xi). \quad (28)$$

Convergence of the solution is controlled by

$$A_{n+2} = -\frac{(n+1)\Lambda\mu_\phi\alpha_\phi b}{(n+2)(1+\Lambda\mu_\phi\alpha_\phi a)} A_{n+1} + \text{(strongly convergent terms)},$$

and the arguments outlined for bending apply here.

For the limiting case of zero rotation speed (27) degenerates to the classic torsion beam functions [5].

$$F_1 = \cos(\gamma_1 x), \qquad F_2 = \sin(\gamma_1 x), \qquad \gamma_1 = \omega\sqrt{\frac{mk_m^2}{GJ}}.$$

4. PROGRAMMING CONSIDERATIONS

Beam functions $F_i(\xi)$ can be treated as known functions by constructing FORTRAN function sub-programs of (22) and (27) using (21) and (26). For a simple cantilever, satisfaction of boundary conditions yields a small set of algebraic homogeneous equations (four for bending, two for torsion), and for constants C_i to be non-zero the determinant must vanish. Hence a simple interval halving method is used to search a predefined range for the discrete real values of ω_j which satisfy the frequency equation. Actual rotor blades are seldom uniform, and often consist of a root region followed by a slightly tapered blade having perhaps one or more balance weights. In most cases this can be idealized as an assembly of uniform segments, and concentrated inertias as shown in Fig. 3.

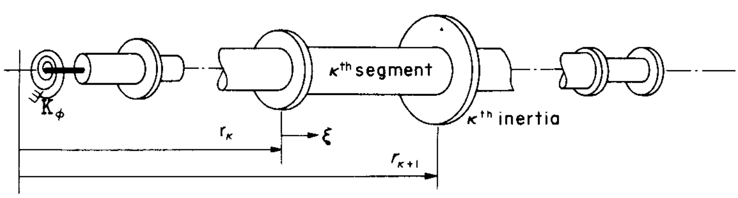

Fig. 3. Nonuniform blade of uniform segments.

For such chained assemblies it is convenient to employ a transfer matrix method [10], to relate the free end to the fixed end conditions. By placing generalized deflections and forces in a state vector

$$\mathbf{z} = \{\mathbf{d}, \mathbf{f}\}$$

they can be related to the undetermined constants C_i for the jth element by a square matrix $\mathbf{B}$,

$$\mathbf{z}_k(\xi) = \mathbf{B}_k(\xi)\mathbf{a}_k, \qquad \mathbf{a}_k = \{C_i\}_k. \quad (29)$$

For bending the state vector contains deflection, bending slope, moment and lateral force; for torsion only deflection and torque:

$$\begin{aligned} \mathbf{z}^v &= \{v, dv_b/dx \,\vdots\, M_\zeta, V_\eta\}, \\ \mathbf{z}^w &= \{w, dw_b/dx \,\vdots\, -M_\eta, V_\zeta\}, \\ \mathbf{z}^\phi &= \{\phi \,\vdots\, M_x\}. \end{aligned} \tag{30}$$

Dimensional quantities are retained in (30) as this facilitates matching the boundary conditions between segments. Usually only the bending component of slope can be equated. Explicit expressions for the components of **B** are given in the Appendix.

State vector transfer proceeds from one end of the blade to the other end, and the centrifugal force in the k-th segment is represented as

$$\tau(\xi) = a_k + b_k\xi + c_k\xi^2, \qquad 0 \leqslant \xi \leqslant 1,$$

$$a_k = \frac{1}{m_k l_k} \sum_{j=k}^{n} m_j l_j (r_j + l_j/2) + M_j r_{j+1},$$

$$b_k = -r_k/l_k, \qquad c_k = -\tfrac{1}{2}, \qquad l_k = r_{k+1} - r_k.$$

If $\mathbf{z}_k(0)$ and $\mathbf{z}_k(1)$ are the state vectors at the beginning and the end of the kth segment, elimination of $\mathbf{a}_k$ in (29) yields

$$\mathbf{z}_k(1) = \mathbf{B}_k(1)\,\mathbf{B}_k^{-1}(0)\,\mathbf{z}_k(0) = \mathbf{U}_k\mathbf{z}_k(0) \tag{31}$$

where $\mathbf{U}_k$ is the transfer matrix over the kth segment. Transfer over the kth inertia is done with the matrix $\mathbf{P}_k$ (see Appendix),

$$\mathbf{z}_{k+1}(0) = \mathbf{P}_k\mathbf{z}_k(1) \tag{32}$$

Hence the state vector at any point can be expressed in terms of the root or initial vector $\mathbf{Z}_R(0)$; at the tip,

$$\mathbf{z}_T(1) = \mathbf{D}\mathbf{z}_R(0), \qquad \mathbf{D} = \prod_{k=1}^{n} \mathbf{P}_k\mathbf{U}_k. \tag{33}$$

The boundary conditions are now imposed and (33) is partitioned into displacement and force parts,

$$\begin{bmatrix} \mathbf{d}_T \\ \mathbf{f}_T \end{bmatrix} = \begin{bmatrix} \mathbf{D}_{dd} & \mathbf{D}_{df} \\ \mathbf{D}_{fd} & \mathbf{D}_{dd} \end{bmatrix} \begin{bmatrix} \mathbf{d}_R \\ \mathbf{f}_R \end{bmatrix}. \tag{34}$$

For a cantilever blade $\mathbf{f}_R$ is always zero. For bending $\mathbf{d}_R^v$, $\mathbf{d}_R^w$ are also zero, whereas inclusion of root torsion requires that

$$f_R^\phi = K_\phi d_R^\phi. \tag{35}$$

Hence the frequency equation for bending is the determinant

$$|\mathbf{D}_{ff}^{v,w}| = 0, \tag{36}$$

and for torsion a scalar expression is obtained,

$$D_{fd} + D_{ff}^\phi K_\phi = 0. \tag{37}$$

Application of the search technique isolates the frequencies, and for every ω_j the mode shapes can be constructed by the sequential application of (31) and (32) starting with the root state vector. For bending the unknown $\mathbf{f}_R$ is the solution of $\mathbf{D}_{ff}^{v,w}\mathbf{f}_R = \mathbf{0}$.

For torsion (35) requires that an arbitrary value be assigned to the now scalar f_R^{ϕ}. Normalization of mode shapes is performed with the usual inner product.

5. APPLICATIONS

To evaluate the method and the general behaviour of rotating beams, a study presented in [1] was made with a uniform cantilever with matched stiffnesses. It showed that the effect of rotation is to produce a dominant increase in the first flap frequency, but only a limited increase in lag. At higher frequencies the difference between flap and lag, and the effect of rotation diminish. The reduction in frequency due to Timoshenko corrections increases with rotation speed, but remains small, with the exception of first lag frequency. Therefore many analyses have ignored the Timoshenko corrections and derived simple empirical formulae for frequencies of rotating uniform cantilevers. Such formulae [4] were compared to our results [11] and found to be a reliable tool for the first few frequencies.

The power of this present method is illustrated by application to typical rotor blades. First the bending frequencies of a relatively simple blade clamped at the root are shown in Fig. 4.

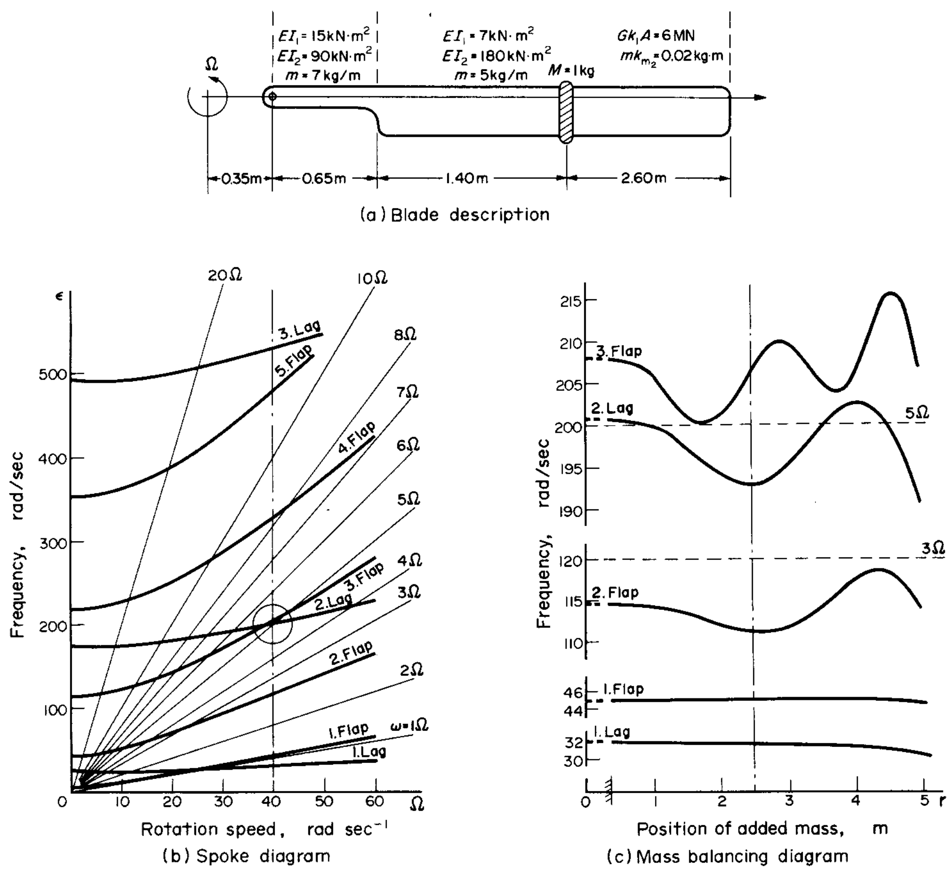

Fig. 4. Bending frequencies of an idealized blade.

The spoke diagram in Fig. 4b shows a potentially dangerous intersection of 2nd lag, 3rd flap and 5Ω excitation at operation speed. By placing a small balancing mass at selected positions, the frequencies can be shifted. Unlike stationary beams, positive shifts of frequency are possible, along with negative shifts, since the stiffening effect of additional centrifugal force can balance and even overcome the effect of increased mass. A complete balancing diagram is shown in Fig. 4c, indicating two positions that would give the safest frequency separation, point A and the tip. The former offers maximum separation from 3Ω and 5Ω resonances and would probably be selected for fatigue and other reasons. A more complex helicopter main rotor is shown in Fig. 5.

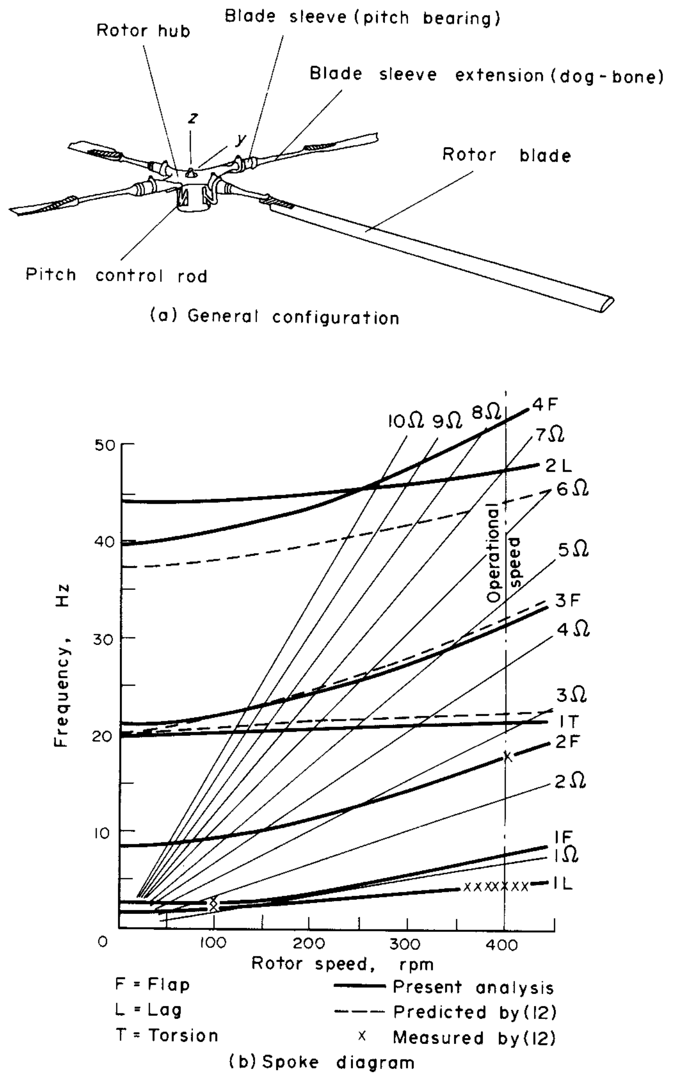

Fig. 5. A practical hingeless rotor system.

The slightly tapered blade is not built-in at the root, but is attached to a complex hub structure which has a significant bending flexibility. Hence the analysis was performed for the whole configuration by considering up to 28 different segments to model the complete structure, from the centre of the hub, through the pitch bearing and the "dog-bone" [12], to the tip of the blade. For torsion a root spring was attached to the end of the pitch bearing to model control system flexibility. The frequencies are presented in Fig. 5(b), and Fig. 6 compares the first non-rotating and rotating modes*. The bending slope, bending moment, shear force, and torque are also shown.

The sharp variations in slope and curvature, present in all plots, are due to the sharp changes in properties near the root. For example, due to its high bending flexibility, the "dog-bone" takes 80% of the total first mode lag bending (Fig. 6(a)). For higher modes these percentages are different. The distribution of bending moment varies radi-

* Full details of blade properties and mode shapes up to the third, in lag, flap and torsion, can be found in [11].

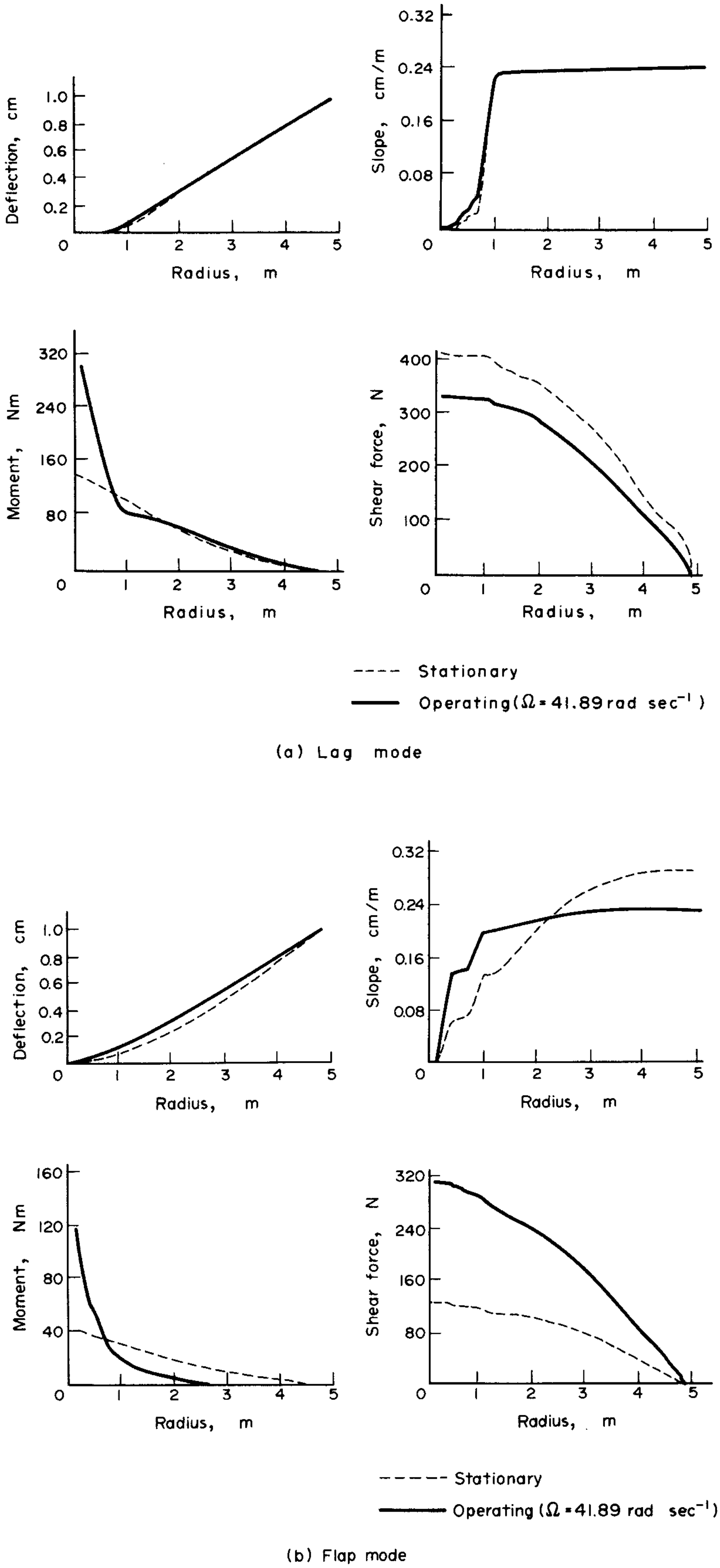

Fig. 6(a) and (b). Mode shapes of the complex blade.

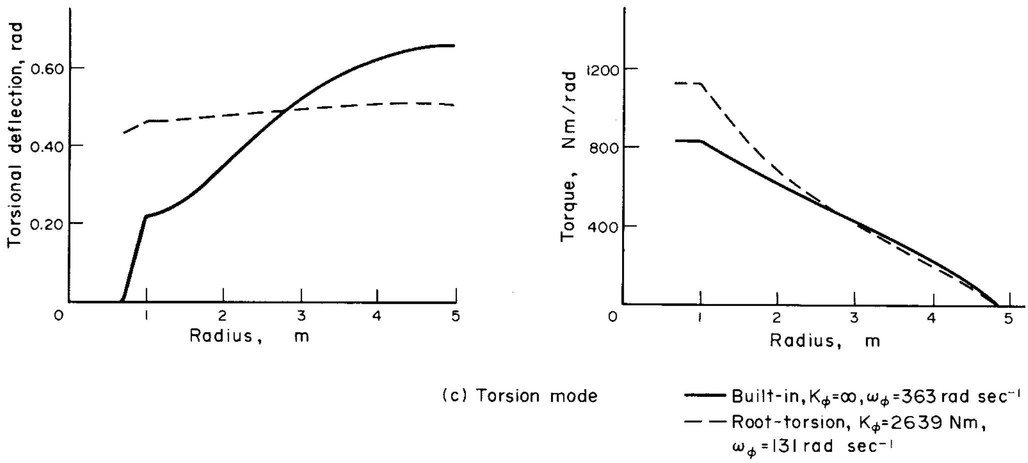

Fig. 6(c). Mode shapes of the complex blade.

cally between non-rotating and rotating configurations. For lag the bending moments at half radius drop with rotation speed from 30% of the total at zero speed to 15% at full speed (Fig. 6(a)). In flap the decrease is from 31% to less than 1% which illustrates the centrifugal relief of soft inplane blades*. For the first rotating flap mode most of the bending takes place over the first 20% of the blade tip radius, but this is not true for higher modes which are much less affected by rotation [11]. The torsional mode is not visibly influenced by rotation speed due to its high stiffness.

The amount of root torsion, chosen such as to match the non-rotating torsional frequency given in [12] considerably diminishes the torsional deformation of the blade.

6. CONCLUSIONS

The principal advantage of this semi-analytic method is the exact representation of centrifugal forces, thus its accuracy is independent of the speed of rotation. Although some of the algebra was lengthy, it is not conceptually difficult and it was a simple matter to include shear deflection and rotatory inertia. In practical applications this approach is attractive for its ease of programming and reliable accuracy over a broad range of parameters. Higher frequencies and mode shapes are computed with equal ease.

Although the problems illustrated here involved some simplification of real rotor systems, it is a relatively simple matter to treat pre-twist and coupled bending. When segments have non-zero pitch angles, transfer from segment to segment is preceeded by a transformation to flap-lag axes. Thus although pitch angle has been ignored in the beam functions of a segment, the centrifugal pitch coupling terms of (11)

$$-m\Omega^2\cos\theta(v\cos\theta - w\sin\theta) \qquad \text{and} \qquad -m\Omega^2[w - \cos\theta(v\sin\theta + w\cos\theta)]$$

are satisfied pointwise at the segment boundaries. Computer programs [9] have been developed for propellers and helicopter rotor blades, and a Users' Manual with a FORTRAN IV listing is available from the authors. Exact treatment of the usual offsets of shear centre and centre of mass require modifications of the equations [2] and transfer matrices.

A second advantage of these methods is the ability to calculate accurate higher derivatives for complex blades. Most other methods employ finite differences [13], or inter-

*According to their lag frequency, rotor blades can be either (a) stiff inplane when $\omega_v > \Omega$, or (b) soft inplane when $\omega_v < \Omega$.

polation functions (e.g. Galerkin methods [2], or finite element solutions [3]). They usually obtain moments and shear forces by numerical differentiation, and the results are well known to be inaccurate [14].

Under certain conditions a type of orthogonality of mode shapes can be established, and numerical integration has confirmed this for realistic blades. These mode shapes have been used as the trial functions in a Galerkin solution of shaft-fixed nonlinear dynamic stability [11], and because of their orthogonality, satisfaction of the linear free vibration equations and accuracy, quite simple and rapidly convergent equations were obtained.

Acknowledgement—We are indebted to Westland Helicopters Limited for supplying the data for the blade in Fig. 5.

REFERENCES

1. R. O. Stafford & V. Giurgiutiu, Semi-analytic methods for rotating Timoshenko beams. *Int. J. mech Sci.* **17**, (1975).
2. J. C. Houbolt & W. Brooks, Differential equations of motion for combined flapwise bending, chordwise bending, and torsion of twisted, nonuniform rotor blades. NACA Rep. 1346 (1958).
3. A. J. Sobey, Dynamical analysis of shaft-fixed helicopter blade. R.A.E. TR 73175 (1974).
4. D. A. Peters, An approximate solution for the free vibrations of rotating uniform cantilever beams. NASA TM X-62, 299 (1973).
5. S. Timoshenko, *Vibration Problems in Engineering*. 3rd Edn. Van Nostrand, New York (1966).
6. E. J. Brunelle, Dynamical torsion theory of rods deduced from the equations of linear elasticity. *AIAA J.*, **10**, 4, 524–526 (1972).
7. G. Allen, Some efficient methods for obtaining infinite series solutions of n^{th} order ordinary differential equations. NASA TR R-390 (1972).
8. J. W. Dettman, *Mathematical Methods in Physics and Engineering*. McGraw-Hill, New York (1962).
9. V. Giurgiutiu & R. O. Stafford, Semi-analytic determination of bending frequencies of propeller and helicopter blades. Imperial College Aero Rep. 75-02 (1975).
10. E. C. Pestel & F. A. Leckie, *Matrix Methods in Elastomechanics*. McGraw-Hill, New York (1963).
11. V. Giurgiutiu, Vibrations and dynamic stability of rotor blades. Ph.D. Thesis, Eng. Faculty, University of London (1977).
12. D. E. H. Balmford, Ground and flight test experience with the Westland Scout hingeless rotor helicopter. *Advanced Rotorcraft*, AGARD-CP-121 (1973).
13. W. F. Hunter, Integrating matrix method for determining the natural vibration characteristics of propeller blades. NASA TN-D 6064 (1970).
14. I. S. Berezin & N. P. Zhidkov, *Computing Methods*. Pergamon Press, Oxford (1965).

APPENDIX—TRANSFER MATRICES B AND P

To perform transfer of the state vector over the uniform segments and the concentrated inertias, transfer matrices **B** and **P** are used. Through matrix **B** the generalized deflections and forces at position ξ are expressed in terms of beam functions F_i (ξ) and arbitrary constant C_i. Combining equilibrium equations (4) and expressions for stress resultants (5), leads to expressions of generalized displacements and forces in terms of total deflections. For bending, substitution of solution (24) leads to the following expressions [1] for the elements of **B**.

$$\begin{aligned}
B_{1i}(\xi) &= F_i(\xi),\\
B_{2i}(\xi) &= (1/l)\{\delta(1 + \delta\alpha\tau)v''' + 2\delta^2\alpha\tau' F_i''(\xi)\\
&\qquad + [1 + \delta^2(\lambda + \underline{\alpha} + \alpha\tau'')]v'\}/[1 - \mu\delta(\lambda + \alpha)],\\
B_{3i}(\xi) &= (EI/l^3)[(1 + \delta\alpha\tau)F_i''(\xi) + \delta\alpha\tau' F_i'(\xi) + \delta(\lambda + \underline{\alpha})F_i(\xi)],\\
B_{4i}(\xi) &= (EI/l^3)\{(1 + \delta\alpha\tau)F_i'''(\xi) + 2\delta\alpha\tau' F_i''(\xi)\\
&\qquad + [\delta(\lambda + \underline{\alpha}) + \mu(1 + \delta\alpha\tau)(\lambda + \alpha) - \alpha(\tau - \delta\tau'')]F_i'(\xi), \quad i = 1,2,3,4
\end{aligned} \tag{A1}$$

where $F_i(\xi)$ is given by (22). The constants in (A1) were not given subscripts, but they should be chosen as appropriate to either lag or flap. Omission of the terms underlined in (A1) is required for flap. For torsion the use of functions (27) and solution (28) yields the simpler expressions

$$\begin{aligned}
B_{1i}(\xi) &= F_i(\xi)\\
B_{2i}(\xi) &= (GJ/l)(1 + \tau\Lambda\alpha_\phi\mu_\phi)F_i'(\xi), \qquad i = 1, 2.
\end{aligned} \tag{A2}$$

The matrix **P** enables the matching of generalized displacements and forces at the segment boundaries with concentrated inertias. Considerations of geometric continuity, and of d'Alembert equilibrium leads to the following expressions for bending

$$\mathbf{P} = \begin{bmatrix} 1 & 0 & 0 & 0 \\ 0 & 1 & 0 & 0 \\ 0 & 0 & 1 & 0 \\ -M(\underline{\Omega^2} + \omega^2) & 0 & 0 & 1 \end{bmatrix} \tag{A4}$$

where for flap the term underlined is omitted. Similar derivation for torsion yields

$$\mathbf{P} = \begin{bmatrix} 1 & 0 \\ M(K^2\omega^2 - K_{12}^2\Omega^2) & 1 \end{bmatrix}, \tag{A5}$$

where K^2 and K_{12} are expressed in terms of inertial principal radii of gyration K_1 and K_2,

$$K^2 = K_1^2 + K_2^2, \qquad K_{12} = K_2^2 - K_1^2.$$